EUROPHYSICS LETTERS 15 October 1990

Europhys. Lett., **13** (4), pp. 313-318 (1990)

Helical Smectic A.

O. D. LAVRENTOVICH[1], YU. A. NASTISHIN[2], V. I. KULISHOV[1], YU. S. NARKEVICH[3] A. S. TOLOCHKO[1] and S. V. SHIYANOVSKII[4]

[1] *Institute of Physics, Academy of Sciences of the Ukrainian SSR pr. Nauki 46, Kiev 252028, USSR*
[2] *L'viv State University - ul. Dragomanova 19, L'viv 290005, USSR*
[3] *Organic Intermediates & Dyes Institute - Moscow 103787, USSR*
[4] *Institute for Nuclear Research, Academy of Sciences of the Ukrainian SSR pr. Nauki 47, Kiev 252028, USSR*

(received 8 March 1990; accepted in final form 2 August 1990)

PACS. 61.30 – Liquid crystals.

Abstract. – A new liquid-crystalline phase has been discovered in a broad temperature region between the cholesteric and smectic-A phases for the mixture of cholesterylnonanoate and nonyloxybenzoic acid. This phase is a helical smectic A with local smectic ordering, helical macrostructure, significant rigidity in shear deformations and ability for formation of nonspherical dispersed drops.

Recognizing the similarity in the role of the phase of the layers in smectic A (SmA) and the phase of the wave-function in superconductors, de Gennes has constructed a Landau-Ginzburg free energy to describe the SmA-nematic phase transition in liquid crystals (LC) [1]. The LC analog of an external magnetic field in a metal is the field of the twist or bend deformations. Thus, the cholesteric, or twisted nematic (N*) phase is the analog of a normal metal in an external magnetic field, and the N*-SmA transition can be described analogously to the metal-superconductor transition in an external magnetic field. The detailed phase diagram depends on the Ginzburg parameter κ, which in LC is equal to the ratio of the twist penetration length to the SmA correlation length.

In type-II superconductors with $\kappa > 1/\sqrt{2}$ in an external magnetic field the Abrikosov flux lattice phase intervenes between the superconducting phase and normal metal [2]. Just as magnetic flux can penetrate type-II superconductor in a lattice of vortices, the twist deformations can be incorporated into SmA by the network of dislocations [1, 3]. As a result, the LC analog of the Abrikosov phase in a form of helical SmA (SmA*) can occur between the N* and SmA phases. Rénn and Lubensky have predicted [3] that this new LC phase is constructed from rotated blocks of usual SmA layers. Mutual rotations of blocks are provided by the network of screw dislocations [3] or fluidlike regions [4]. The helical axis of SmA* is parallel to the planes of smectic layers and perpendicular to the long axes of molecules.

Until now, as far as we know, the existence of the SmA* phase between the N* and SmA phases has not been proved experimentally. Alternatively, Goodby *et al.* [5] have recently reported the observation of SmA* in the case of the isotropic liquid-to-chiral smectic C transition.

Our purpose is to find the SmA* phase in the case of the N*-SmA transition. A mixture of cholesteryl-*n*-nonanoate (CN) and *n*-nonyloxybenzoic acid (NOBA) in weight proportion 7 : 3 was investigated. The choice was caused by the earlier observation [6] of the anomalous elongation and division of the dispersed LC drops in the N*-SmA pretransitional region. The interpretation of these phenomena had been based on the suggestion, that just in this material $\kappa > 1/\sqrt{2}$, see ref. [6].

We have used optical methods to distinguish SmA* from SmA (sect. 1) and the X-ray method to distinguish SmA* from N* (sect. 2). Further evidences were obtained from calorimetrical and acoustical data, as well as from the peculiarities of the drop shape, sect. 3, 4, 5, respectively. In all experiments the mixture was cooled from the isotropic state (clearing point 105 °C) down to the solid crystalline state (solidification point 58 °C) at a rate (0.5 ÷ 2) °C/min.

1. Optical properties.

The mixture textures in flat glass cells with thickness 50 μm and normal boundary conditions for the director orientation were examined using a polarizing microscope. The mixture possesses textures typical of SmA homeotropic (pseudoisotropic) [7] within the temperature range $58 \leqslant T \leqslant 82.6$ °C and the fingerprint texture with light and dark bands at $T \geqslant 82.6$ °C. The latter is typical for the helical LC structures with axis in the plane of cell [7]. Rotations between crossed polarizers of this texture produce extinction in the cases when the bands are parallel either to analyser or polarizer. This means that the helix axis is perpendicular to the director, which is obvious for the N* phase and expected for the SmA* phase [3].

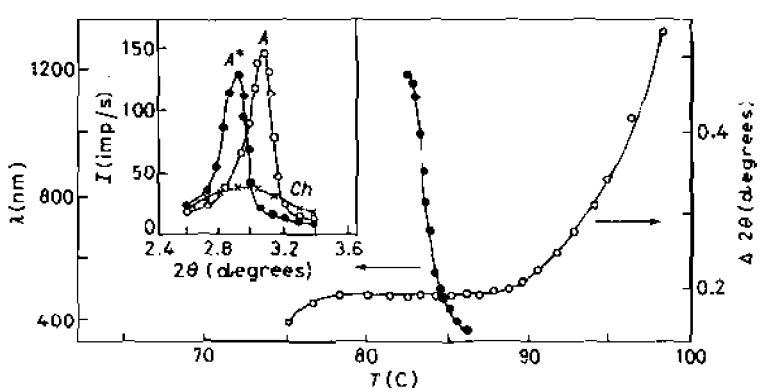

Fig. 1. – Temperature dependence of the maximum wavelength λ of the selective reflection (closed circles) and half-width of the X-ray diffraction peaks for CN : NOBA mixture. The inset shows scans through the peak at temperatures within the SmA phase (open circles, $T = 75$ °C), the SmA* phase (closed circles, $T = 86$ °C), and the N* phase (crosses, $T = 97$ °C).

In cells with tangential anchoring the typical planar N* textures were observed within the range $82.6 \leqslant T \leqslant 104$ °C. Rotation between the polarizers produced no extinction, which is again a typical feature of the helical structure [7].

In addition, the helical structure of mixtures for $T \geqslant 82.6$ °C has been confirmed by transmittance spectra in the Bragg diffraction region, fig. 1. The spectra have been obtained

on the tangentially anchored samples. The error in the absolute value of the maximum wavelength λ of the selective reflection was estimated to be 1%. Cooling resulted in the increasing of λ and, consequently, in the unwinding of the helix. This unwinding is also clearly visible in the textures.

Thus, optical data unambiguously confirm the existence of the SmA phase at $T \leqslant 82.6\,^{\circ}C$ and the helical phase, N* or/and SmA*, at $T \geqslant 82.6\,^{\circ}C$. It is necessary to note, that the half-width of the optical Bragg peak does not change significantly within the range $82.6 \leqslant T \leqslant 104\,^{\circ}C$. Moreover, there is no temperature hysteresis of λ within this range. These facts confirm the absence of the phase separation of the mixture. In addition, we could not find any manifestations of this separation in the textural observations.

2. X-ray scattering.

Small-angle X-ray measurements were performed for unaligned samples (in 1 mm glass cylindrical capillaries) in the range $2\theta = (0.1 \div 5)^{\circ}$. As the X-ray source, monochromatized CuK radiation was used (30 kV, 30 mA, focus size $(0.4 \times 8)\,mm^2$, X-ray wavelength $\lambda_X = 1.541$ Å). Instrumental resolution was 0.02° in the scan direction.

The temperature dependence of the peak half-width ($\Delta(2\theta)$) is shown in fig. 1. The inset of fig. 1 shows peak scans taken within the SmA phase and two different temperatures within the helix states.

As the temperature is lowered down to 90 °C, the mixture possesses a X-ray signature typical of the N* phase. The intensity of the small-angle peak grows larger and sharpens up, as described by many authors for the N* phase in the vicinity of the N*-SmA transition, see, *e.g.*, ref. [8, 9].

For $T \leqslant 90\,^{\circ}C$, the X-ray pattern is typically smecticlike. This region is characterized by the sharp diffraction peak of high intensity similar to that observed for SmA by others [8, 9]. The peak angular position ($2\theta = 2.92^{\circ}$) and half-width are practically constant within the broad range $78 \leqslant T \leqslant 90\,^{\circ}C$. One can estimate the correlation length $\xi_{\parallel}$ of the smectic ordering within this range by using the Sherrer formula $\xi_{\parallel} = \lambda_X/\Delta(2\theta)\cos(2\theta/2)$. The estimation yields $\xi_{\parallel} = (450 \div 500)$ Å, which implies that layer correlations extend over a minimum distance of $15 \div 20$ layers. Thus, the smectic layering is a key element of the structure at $T \leqslant 90\,^{\circ}C$.

Comparison of the optical and X-ray data leads to the conclusion that the mixture possesses local SmA ordering at $T \leqslant 90\,^{\circ}C$ and helix structure at $T \geqslant 82.6\,^{\circ}C$. In other words, a new state with helical macrostructure and local smectic ordering intervenes between two usual SmA and N* phases, exactly as predicted for the SmA* phase [3].

3. Thermodynamical properties.

Differential scanning calorimetry gives evidence, that properties described above are manifestation of the new SmA* phase rather than the pretransitional effects in the N* phase. There are two peaks, narrow and broad, on the DSC trace, fig. 2. The narrow one with latent heat 1.03 kJ/mol corresponds to the clearing point. The broad peak with total latent heat 0.27 kJ/mol and starting point of growth approximately at 91 °C is located within the region of the helix states. This peak is unambiguously separated from the point transition to the SmA phase at 82.6 °C, which was detected by optical methods. It is natural to connect this peak with the N*-SmA* phase transition.

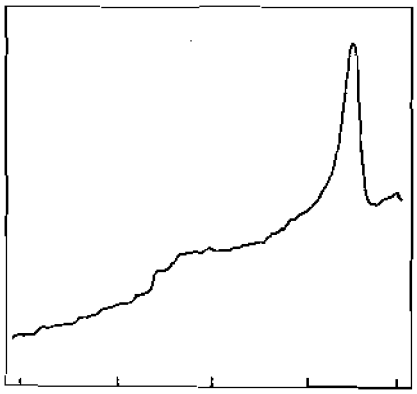

Fig. 2.

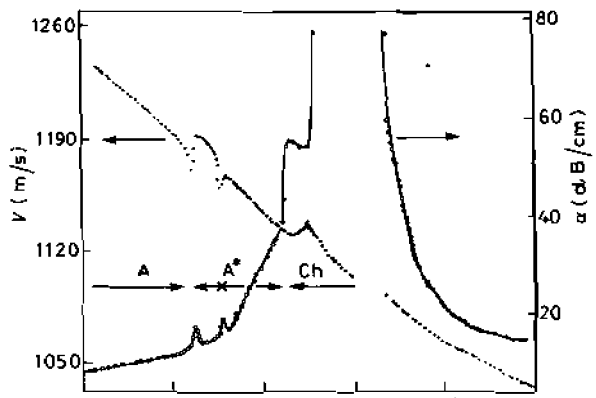

Fig. 3.

Fig. 2. – DSC trace of CN:NOBA mixture. DSC-111, sample weight 88.1 mg.

Fig. 3. – Temperature dependence of the velocity V and attenuation α of the longitudinal ultrasound of frequency 5 MHz in CN:NOBA mixture.

4. Acoustic probing.

The velocity and attenuation of the longitudinal ultrasound of frequency 5 MHz were measured in the unoriented samples as a function of the temperature. The phase-matching technique, which is similar to that described in ref. [10], was employed. The velocity measurements were accurate to 10^{-3}% and the attenuation measurements were accurate to 10%. As follows from the data (fig. 3), the SmA-SmA* and SmA*-N* transitions are clearly visualized by the velocity minima and the attenuation maxima. Moreover, there is an additional peak inside the SmA* region, which indicates that the SmA* phase may contain different states.

Unusual rheological properties of the SmA* phase in comparison with the SmA and N* phases were manifested in shear deformation experiments. The mixture was placed between two glass plates. The upper one was moved in the plane of the cell with frequency 230 Hz. The lower plate was fixed. The amplitude Δx of the upper plate vibrations was measured using a vibrometer. The vibration amplitude tends to 0 in the solid crystalline state ($T \leqslant 58$ °C) as well as in the SmA* phase, fig. 4. This phenomenon does not depend on the character of the initial LC orientation. For pure CN this effect is not observed, fig. 4. We suggest that the lattice structure of the SmA* phase may be responsible for the rigidity of this state and, as a result, for decreasing Δx.

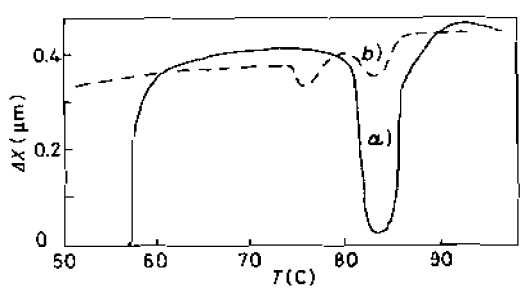

Fig. 4. – Temperature dependence of the amplitude of the plate vibrations in the cell with CN:NOBA mixture (*a*)) and pure CN (*b*)).

5. Shape of the freely suspended drops.

Further evidence for distinguishing the SmA* phase from the N* and SmA phases and for the validity of the lattice model of SmA* was obtained from the investigations of dispersed LC drops. Drops with radii $(1 \div 100)\,\mu$m were dispersed in glycerine to which small amounts (up to 1 wt.%) of lecithin were added in order to create the normal boundary conditions. The N* and SmA drops are spherical within the whole temperature ranges of these phases. Alternatively, the equilibrium shape of the SmA* drops is nonspherical, namely, spindlelike within the range $82.6 \leqslant T \leqslant 85.6\,^{\circ}$C and pyramidal at $85.6 \leqslant T \leqslant 92\,^{\circ}$C. All transitions between the drops of different shape are reversible and reproducible. It is important to note that point 85.6 °C of the spindlelike-pyramidal transformation of shape coincides with the position of the additional peaks in acoustical data, fig. 3.

The shape of the drops, which are dispersed in the isotropic liquid, is determined by the ratio of the volume energy F_v to the surface energy F_s. Here F_v is the energy of the elastic deformations in a drop and F_s is determined by the surface tension σ ($F_s \sim \sigma\pi R^2$). The latter was measured separately using a pendant drop method [11]: in the N* and SmA phases the LC-matrix interface gives $\sigma \approx 10^{-2}\,\mathrm{J/m^2}$ and in SmA* $\sigma \approx 3 \cdot 10^{-3}\,\mathrm{J/m^2}$.

The estimation of F_v is more complicated due to the different structures of the discussed phases. For normally anchored SmA and N* drops it is natural to assume that $F_v = 8\pi KR$, where K is a curvature modulus and R is the drop radius [12]. Thus, with $K = 10^{-11}$ N typical for N* and SmA and with $R = 10\,\mu$m, $\sigma = 10^{-2}\,\mathrm{J/m^2}$, one finds $F_v/F_s \sim 10^{-3}$. Therefore nonspherical drops are impossible in the N* and SmA phases. However, the situation may be drastically changed for the SmA* drops.

If SmA* consists of a regular array of twist grain boundaries [3], one can expect that F_v is determined by the deformations of this lattice with some compression elastic modulus B: $F_v \sim BR^3$. Thus for the SmA* drops, $F_v/F_s \sim BR/\sigma$, rather than $\sim K/R\sigma$, as for the N* and SmA drops. Modulus B can be roughly estimated as K/Pd, where P is a helix pitch of SmA* and d is a molecular length. For typical $P = 400$ nm and $d = 30$ Å one obtains $B = 10^4\,\mathrm{N/m^2}$. This leads to $F_v/F_s \sim 10$ in the SmA* drops, which naturally explains the drop nonsphericity.

It is important to note that the nonsphericity cannot be explained by phase separation inside the drop. Such a hypothetical separation, which is accompanied by the formation of the usual Sm and N* regions, must lead to a shape with sphericallike surfaces (fig. 5*a*)), because for any part of such a heterogeneous drop $F_s \gg F_v$. Alternatively, in the experiment, the SmA* drops possess a cylindrical shape rather than combined spherical one (fig. 5*b*), *c*)). In the SmA*-SmA pretransitional region, the SmA section of drop assumes a

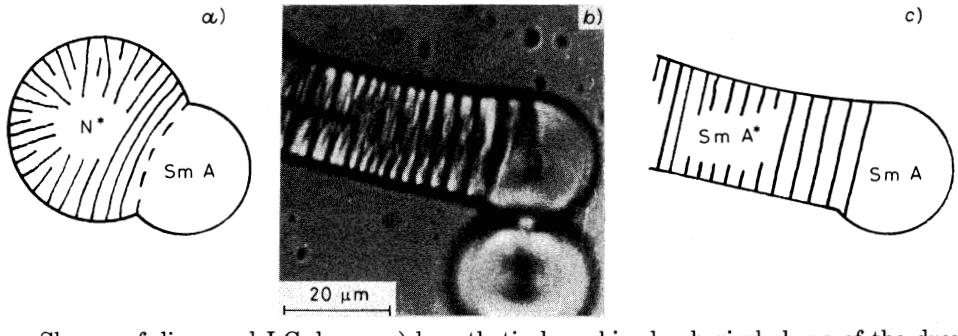

Fig. 5. – Shapes of dispersed LC drops: *a*) hypothetical combined spherical shape of the drop with phase separation of mixture and coexisting N* and SmA regions; *b*) microphotography of the cylindrical SmA* drop with semispherical SmA region, $T = 82.6\,^{\circ}$C; *c*) the schematic representation of *b*).

semispherical shape (here $F_s \gg F_v$) and the SmA* section is cylindrical due to the fact that this geometry conserves the undistorted SmA* helical structure inside the drop volume (here $F_s < F_v$). The layers of the helical structure are parallel to each other and everywhere oriented perpendicular to the surface, as is evident in fig. 5*b*) because of the increase in the helix pitch in the pretransitional region.

Conclusion.

Comparison of all independent data described above confirms the existence of the new SmA* phase within the broad temperature range, which is clearly distinguished from the SmA and N* phases. The CN:NOBA mixture exhibits the following phase diagram:

crystal (58 °C) SmA (82.6) SmA* (≈90) N* (105 °C) isotropic liquid.

The SmA* phase possesses simultaneously the local smectic ordering and the helical macrostructure. Furthermore, SmA* exhibits some properties unusual for LC phases, namely, a significant rigidity in shear deformations and in the drop formation, which can be caused by the regular array of grain boundaries composed of dislocations [3] or fluidlike regions [4]. The periodic macrostructure of SmA* may lead to concentration waves for the components of the mixture with the space period of the dislocation (or fluidlike) lattice. The latter as well as polymorphic transitions in the dislocation array may be responsible for the existence of different states within the SmA* region, which seems to be visible in the data obtained. However, usual phase separation in the sense of a nonperiodical distribution of components is not observed.

* * *

We are grateful to V. A. LINJOV, A. P. POLISHCHUK, V. V. SERGAN, L. N. TARAKHAN for help in experiments and to E. I. DEMIKHOV for fruitful discussion. We also are grateful to the referee for the information about ref. [4].

REFERENCES

[1] DE GENNES P. G., *Solid State Commun.*, **10** (1972) 753.
[2] ABRIKOSOV A. A., *Ž. Èksp. Teor. Fiz.*, **32** (1957) 1442 (*Sov. Phys. JETP*, **5** (1957) 1174).
[3] RENN S. R. and LUBENSKY T. C., *Phys. Rev. A*, **38** (1988) 2132.
[4] TONER J., unpublished paper.
[5] GOODBY J. W., WAUGH M. A., STEIN S. M., CHIN E., PINDAK R. and PATEL J. S., *Nature (London)*, **337** (1989) 449; *J. Am. Chem. Soc.*, **111** (1989) 8119; LEE S.-D., PATEL J. S., GOODBY J. W. and WAUGH M. A., *Phys. Lett. A*, **139** (1989) 71; PINDAK R. *et al.*, *Phys. Rev. Lett.*, **64** (1990) 13.
[6] LAVRENTOVICH O. D. and NASTISHIN YU. A., *Pis'ma Ž. Èksp. Teor. Fiz.*, **40** (1984) 242 (*JETP Lett.*, **40** (1984) 1015).
[7] DEMUS D. and RICHTER L., *Textures of Liquid Crystals* (VEB Deutscher Verlag für Grundstoffindustrie, Leipzig) 1980.
[8] MCMILLAN W. L., *Phys. Rev. A*, **6** (1972) 936.
[9] WENDORFF J. H. and PRICE F. P., *Mol. Cryst. Liq. Cryst.*, 24 (1973) 129.
[10] MIANO K. and KETTERSON T., *Phys. Rev. A*, **12** (1975) 615.
[11] LAVRENTOVICH O. D. and TARANKHAN L. N., *Ž. Tekhn. Fiz.*, **56** (1986) 2071.
[12] LAVRENTOVICH O. D. and TERENT'EV E. M., *Ž. Èksp. Teor. Fiz.*, **91** (1986) 2084 (*Sov. Phys. JETP*, **64** (1986) 1237).